Letters in Applied NanoBioScience
Open-Access Journal (ISSN: 2284-6808)

Article
Volume 12, Issue 4, 2023, 137
https://doi.org/10.33263/LIANBS124.137

Organic Chromophores from D–π–A to D–A'–π–A: Influence of the Auxiliary Acceptor on Energy Levels, Molecular Absorption, and Nonlinear Optical Response

Ahmed Azaid [1,*], Tayeb Abram [2], Rchid Kacimi [2], Marzouk Raftani [1], Youness Khaddam [1], Diae Nebbach [1], Abdelouahid Sbai [1], Tahar Lakhlifi [1], Mohammed Bouachrine [1,3,*]

[1] Molecular Chemistry and Natural Substances Laboratory, Faculty of Sciences, University Moulay Ismail, Meknes, Morocco
[2] MEM (LASMAR) ESTM, University Moulay Ismail, Meknes, Morocco
[3] EST Khenifra, Sultan Moulay Sliman University, Beni mellal, Morocco
* Correspondence: m.bouachrine@est-umi.ac.ma (M.B.); a.azaid@edu.umi.ac.ma (A.A.);

Scopus Author ID 8983993500
Received: 2.04.2022; Accepted: 16.05.2022; Published: 8.10.2022

Abstract: In this research article, four organic chromophores of type D–Ai–π–A (i=2–4) combining various auxiliary acceptors (Ai) with phenothiazine (PTZ) as the electron donor, thiophene as the π-conjugated bridge, and tricyanovinyl dihydrofuran (TCF) as the electron acceptor have been structured and theoretically studied using density functional theory (DFT) and time-dependent DFT (TD-DFT) methods. The effects of various auxiliary acceptors in D–Ai–π–A chromophores on the nonlinear optical (NLO) response have been examined. In this context, the geometric and electronic structures, intramolecular charge transfer (ICT), NBO analysis, absorption wavelength in different organic solvents, polarizability (α), and hyperpolarizability (β) have been determined. They have been assessed to predict the appropriate candidates for NLO material. The data obtained illustrate that all chromophores with various auxiliary acceptors present a large NLO response ranging from 13541.17 to 66723.38 (a.u), PTZ-2 especially with auxiliary acceptor 2,3-dimethylthieno[3,4-b]pyrazine presents the highest <a> [(879.10 (a.u)) and βtot (66723.38 (a.u)] values. A strong NLO response indicates that this series of organic chromophores with a D-Ai-π-A architecture exhibits large first hyperpolarizability βtot values, which are much greater than those of urea.

Keywords: phenothiazine; tricyanovinyl dihydrofuran; NLO; TD-DFT; D–π–A; D–A'–π–A.

1. Introduction

The promising nonlinear optical (NLO) materials have attracted considerable interest in current research [1] due to their viable application in optoelectronic devices, optical data storage, optical switching, optical information processing, optical power limiting applications [2-3], utilization in the fields of solid-state physics, interface physics, medicine, chemical dynamics, materials science and other fields [45]. Among different materials, organic materials have been examined as a feasible alternative to inorganic compounds due to their low cost, facile fabrication, synthesis, structural modification with suitable substituents, low dielectric constant, and large nonlinear response [67]. Organic NLO molecules with donor (D) and acceptor (A) groups coupled via π-spacers exhibit a nonlinear optical response due to the molecular polarizability of nonlocalized π-electron under the influence of a light field [89]. Indeed, the NLO response of organic materials is stronger and faster than that of inorganic

materials due to the movement of the nonlocalized π-electron, which is easy and not affected by lattice vibrations [10]. Therefore, the increased intramolecular charge transfer (ICT) reinforces the NLO response properties, whereas charges are delocalized from donor (D) to acceptor (A) groups through π-spacer [11]. In general, metal-free organic compounds consist primarily of three elements: donor (D), π-spacer (π), and acceptor (A). On this basis, several organic molecular architectures (D-A, D-A-π-A, D-π-A, D-π-D-π-A, D-π-A–π-D, D-π-π–A, and D–D–π–A, etc.) have also been created to achieve high power efficiency [1213]. To increase the light-harvesting capabilities of organic chromophores with a similar structure of D-π-A, an auxiliary acceptor was introduced in the conjugated bridge between the electron donor and the π-bridge to form a D–A′–π–A type structure [1415]. Indeed, different kinds of electron-withdrawing groups such as phthalimide [16], benzothiadiazole [1718], benzotriazole [19], quinoxaline [2021], and diketopyrrolopyrroles [2223] have been used as the auxiliary acceptor for viable D−A−π−A structures. Recently, a novel chromophore PTZ-1 with the architecture D-π-A was synthesized by Yuhui Yang *et al*. [24]. This chromophore contains the phenoxazine (PTZ) and tricyanofuran (TCF) acceptor linked together via thiophene as the π-conjugated bridge figure 1. It was proposed that this chromophore may be used in nonlinear optical (NLO) applications.

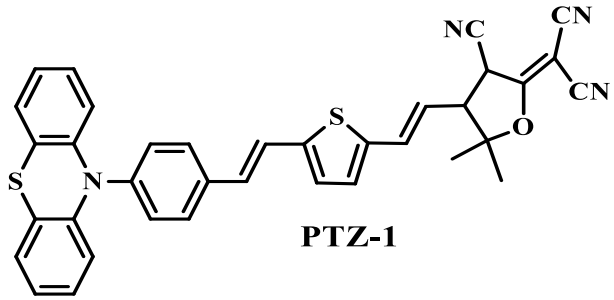

Figure 1. Structure of chromophore PTZ-1.

In this work, we concentrate on developing a D–Ai–π–A architecture; this structure may be produced by inserting an acceptor group denoted Ai betwixt the donor group and the π-linker as just an additional acceptor in the reference architecture (D–π–A). In particular, chromophore PTZ-1 with (D–π–A) structure showed a lower energy gap, good thermal stability, and nonlinear optical properties [24]. Motivated by these characteristics and to aid future experimental research aiming to design effective organic compounds to be used as the nonlinear optical (NLO) chromophore molecule, theoretical quantum computations have been accurate in predicting and estimating the characteristics of the chromophores NLO [25]. Therefore, our objective consists of studying the supplementary acceptor's influence on the geometric, electronic, optical, and nonlinear characteristics. For that reason, three chromophores PTZ-2, PTZ-3, and PTZ-4 of the configuration D–Ai–π–A (i=1–3) were designed from the chromophore PTZ-1, where the donor D is phenothiazine (PTZ), the π-linker is thiophene, the electron acceptor A is tricyanovinyl dihydrofuran (TCF) for all chromophores. In contrast, the additional acceptor is 2,3-dimethylthieno[3,4-b]pyrazine (PTZ-2), benzo[c][1,2,5]thiadiazole (PTZ-3) and [1,2,5]thiadiazolo[3,4-d]pyridazine (PTZ-4) figure 2. Geometric and electronic structure, energy gap, frontier molecular orbitals (FMO), natural bond orbital (NBO) analyses, polarizability (α), and hyperpolarizability (β) were studied by applying density functional theory (DFT). In contrast, the absorption wavelength in different organic solvents is studied using time-dependent DFT (TD-DFT).

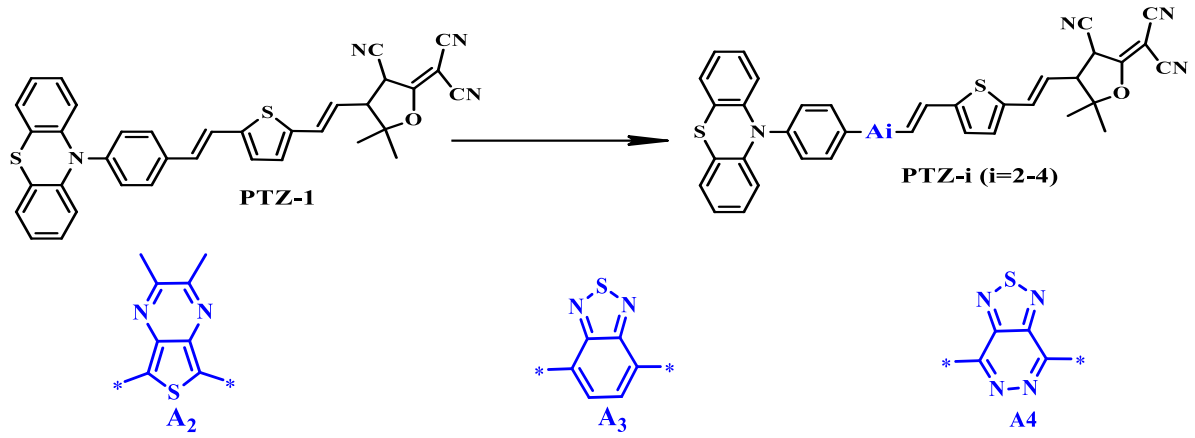

Figure 2. Structures of chromophores PTZ-1- PTZ-4.

2. Materials and Methods

In this research, the DFT computations were carried out using the Gaussian 09 [26] supported by the GaussView 5.1.8 interface for visualization [27], with the exchange-correlation hybrid functional B3LYP [28] and the 6-31G+(d,p) basis set [29]. In the gas phase, the geometry structures of all chromophores were optimized, and the HOMO, LUMO, and HOMO-LUMO gaps energies were calculated [3031]. The computed orbital populations were used to forecast the natural bond orbital (NBO) [32] analysis using the NBO 6.0 software incorporated into the Gaussian 09 package program [26].

For chosen compounds, the absorption spectrum, vertical absorption energies, and oscillator strengths were computed in various organic solvents employing Time-Dependent Density Functional Theory (TD-DFT) [33] with coulomb-attenuated hybrid exchange-correlation functional (CAM-B3LYP) [34]. In addition, we used DFT with the CAM-B3LYP functional, and the basis set 6-31G (d) to study NLO characteristics for chromophores PTZ-1, PTZ-2, PTZ-3, and PTZ-4, such as the polarizability (α) and first hyperpolarizability (βtot). Indeed, the polarizability (α) and the first hyperpolarizability (βtot) are all features that imply their utility as nonlinear optical materials [35-36]. They are computed using the x, y, and z units in equations (1) and (2):

Here, it combines the different quantities:ict

$$< \alpha > = \frac{1}{3}\left(\alpha_{xx} + \alpha_{yy} + \alpha_{zz}\right) \qquad (1)$$

$$\beta_{tot} = \sqrt{\beta_x^2 + \beta_y^2 + \beta_z^2} \qquad (2)$$

Here, $\beta_i = (i = x, y, z)$ combines the different quantities: $\beta_i = (\frac{1}{3})\Sigma_{j=x,y,z}(\beta_{ijj} + \beta_{jij} + \beta_{jji})$

3. Results and Discussion

3.1. Geometric properties.

The optimized geometries of the chromophores PTZ-1, PTZ-2, PTZ-3, and PTZ-4 calculated using DFT/B3LYP/6-31G+(d,p) level are represented in figure 3. Their primary optimized geometrical parameters such as the dihedral angle θi (i = 1–4) and the link distance parameters di (i = 1–4) are collected in table 1 and scheme 1.

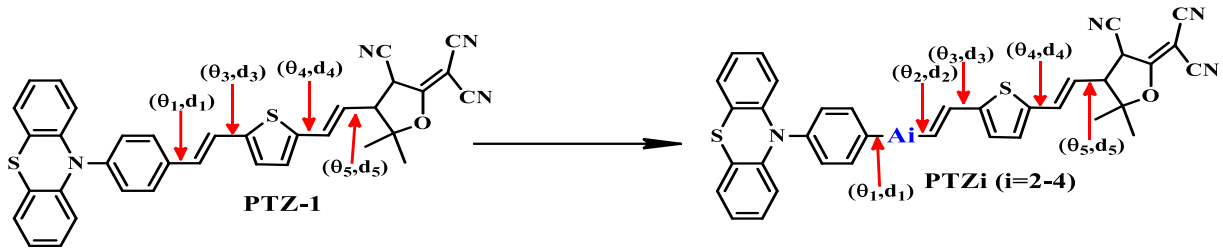

Scheme 1. Studied geometric parameters.

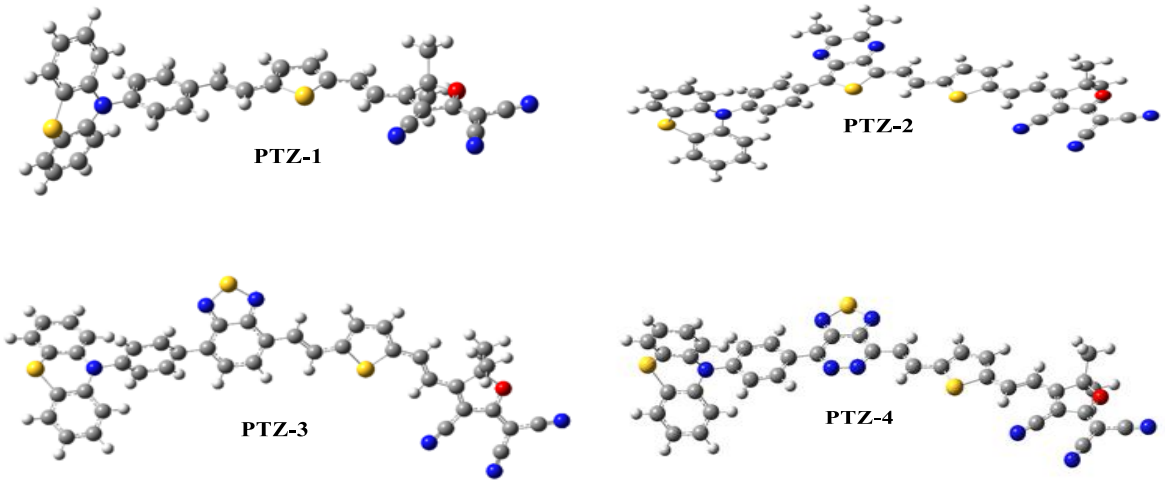

Figure 3. Optimized structures of all studied chromophores (PTZ-1- PTZ-4) using B3LYP/6-31G +(*d,p*) level.

Table 1. Distances di (Å) and dihedral angles θi (°) of the studied chromophores calculated by B3LYP/6-31G +(d,p).

Chromophore	**d1(Å)**	**d2(Å)**	**d3(Å)**	**d4(Å)**	**d5(Å)**
PTZ-1	1.45	***	1.44	1.42	1.42
PTZ-2	1.46	1.42	1.42	1.43	1.42
PTZ-3	1.47	1.45	1.44	1.42	1.42
PTZ-4	1.47	1.45	1.43	1.43	1.42
Chromophore	**θ1(°)**	**θ2(°)**	**θ3(°)**	**θ4(°)**	**θ5(°)**
PTZ-1	178.39	***	178.28	179.70	179.76
PTZ-2	163.36	179.36	179.49	179.63	179.70
PTZ-3	144.99	179.54	179.72	179.89	179.99
PTZ-4	179.96	179.99	179.98	179.99	179.99

All the chromophores are nearly planar with identical dihedral angles θ1, θ2, θ3, and θ4 values close to 180°. A small twist was detected for PTZ-2 and PTZ-3, whose θ1 is around 163.36° and 144.99°, respectively. This may be explained by the existence of a steric hindrance effect between the donor (D) and the auxiliary acceptor groups. For the chromophores examined, the results of the optimized structures indicate that all the chromophores have planar structures. The shortest values estimated lengths di (i=1-4) for all organic chromophores are in the range of 1.42 Å to 1.47 Å; these values are intermediate between the distances of both a single link and a double link. This diminution in length results from the conjugation effect in the systems investigated. This coplanar structure confirms and simplifies intramolecular charge transfer ICT [37].

3.2. Frontier molecular orbital and energy levels of the designed chromophores.

To better understand intramolecular charge transfer (ICT), the electronic distributions of molecular orbital frontiers of four molecules were estimated by applying the B3LYP technique with 6-31G +(d,p) level, which is represented in figure 4. According to the border orbital density of the HOMO electrons in the chromophores studied, the HOMO electrons of

PTZ-1, PTZ-2, PTZ-3, and PTZ-4 are localized in the donor electron fragment. For the distribution of LUMO, the electron density of all chromophores is primarily located on the Ai–π–A part. This demonstrates sufficient electron density separation betwixt the HOMO and LUMO orbitals, which facilitates ICT transitions for all chromophores and demonstrates a decrease in bandgap and a shift in absorption toward the red. Hence, the E_{gap} of all investigated molecules was computed using the following formula: Egap = E_{HOMO} – E_{LUMO} [38] and is reported in table 2. According to this table, the reference chromophore PTZ-1 has gap energy of 1.68 eV. In comparison to PTZ-1, the gap energy decreases in the following order: PTZ-1 (1.68eV) > PTZ-2 (1.59 eV) > PTZ-3 (1.50 eV) > PTZ-4 (1.20 eV).

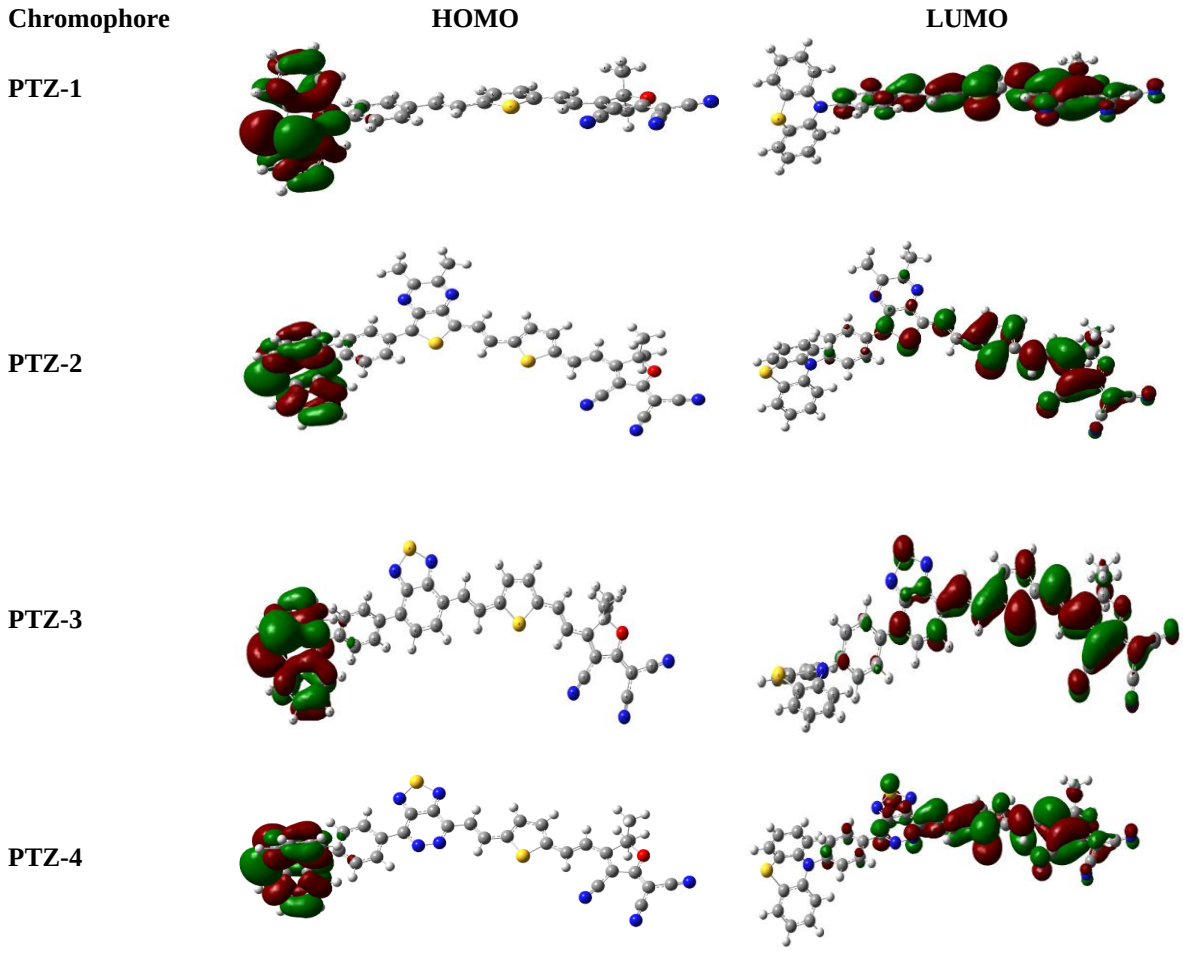

Figure 4. Contour plots of the frontier orbitals of all chromophores.

Table 2. The E_{HOMO}, E_{LUMO}, and gap energies of the tested chromophores.

Chromophore	E_{HOMO} (eV)	E_{LUMO}(eV)	E_{gap}(eV)
PTZ-1	-5.177	-3.497	1.68
PTZ-2	-5.104	-3.512	1.59
PTZ-3	-5.101	-3.601	1.50
PTZ-4	-5.082	-3.877	1.20

3.3. NBO analysis.

To investigate the charge distribution of the D–Ai-π-A (i=2–4) molecular systems, NBO analysis of optimized structures [39] of PTZ-1-PTZ-4 compounds has been estimated employing the DFT-B3LYP/6-31G+(d,p) approach in the gas phase and the results are reported in table 3 using atomic units. For the chromophores PTZ-1 and PTZ-2, the positive NBO charge of donor D, auxiliary acceptor Ai, and π-spacer groups indicates that they are excellent electron-pushing groups (electron donation). The acceptor group A has a negative NBO charge,

indicating that they are efficient electron-withdrawing groups (electron acceptor) that trap the electron in the molecular backbone. On the other hand, the chromophores PTZ-3 and PTZ-4 have positive charges in the donor and π-linker groups, whereas the acceptor and auxiliary acceptor Ai groups have negative charges. Indeed, the positive charges in the bridge reveal that this unit functions as a donor. While the most negative (NBO) charge on the acceptor portion indicates, the best acceptor group for all chromophores investigated.

Table 3. The NBO analysis of all chromophores (PTZ-1- PTZ-4).

Compound	Donating Group	auxiliary acceptor	π- spacer	Acceptor Group
PTZ-1	0.008	****	0.182	-0.190
PTZ-2	0.019	0.027	0.188	-0.234
PTZ-3	0.032	-0.047	0.207	-0.192
PTZ-4	0.058	-0.144	0.274	-0.188

3.4. Molecular electrostatic potential (MEP).

To estimate the reactive areas of the examined chromophore when electrophilic and nucleophilic attacks, as well as hydrogen bonding interactions, we have simulated the MEP [40] of all chromophores using the B3LYP/6-31G+(d,p) level, as illustrated in Figure 5. Different electrostatic potential values are indicated by distinct colors on the MEP surface. While the negative electrostatic potential areas are illustrated in red and correspond to electrophilic reactivity, the most positive electrostatic potential areas are represented by blue and correspond to nucleophilic reactivity. In contrast, the zero electrostatic potential regions are illustrated in green. As depicted in figure 5, the MEP reveals that all chromophores' maximum positive area (blue color) is around the sulfur atoms of the π-spacer group and the auxiliary acceptor. While the negative area (red color) is largely centered around the nitrogen atoms of the TCF groups in all molecules examined.

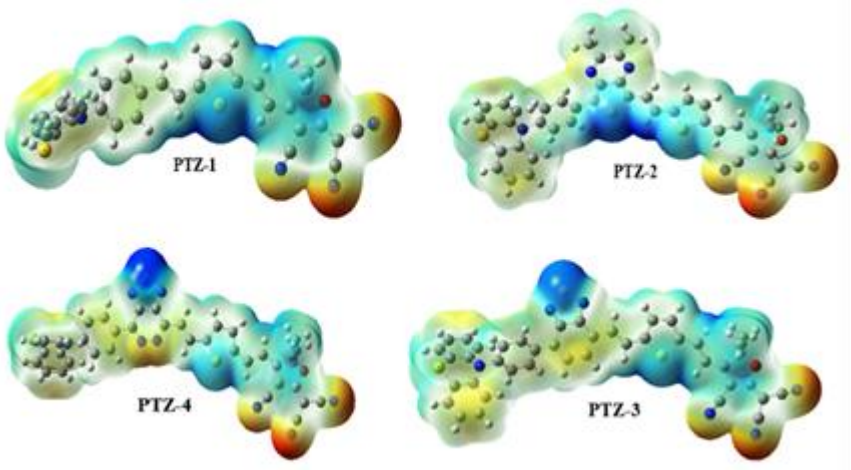

Figure 5. MEP surfaces of the four studied compounds (PTZ-1- PTZ-4).

3.5. Molecular electrostatic potential (MEP).

In chemistry, different concepts have been designed to explain and predict various physicochemical phenomena and offer information on the electronic structure of chemical species [41]. Using the HOMO and LUMO energies (E_{HOMO} and E_{LUMO}), the chemical potential (μ) [42], chemical hardness (η) [4344], softness (S), and electronegativity (χ) [45] are all calculated, and the findings obtained are listed in Table 4. These chemical reactivity indices can be calculated based on the following equations:

$$\text{Chemical hardness: } \eta = \frac{E_{LUMO} - E_{HOMO}}{2} \quad (3)$$

$$\text{Chemical potential: } \mu = \frac{E_{LUMO} + E_{HOMO}}{2} \quad (4)$$

$$\text{Electronegativity: } \chi = -\mu = \frac{-(E_{LUMO} + E_{HOMO})}{2} \quad (5)$$

$$\text{Chemical softness: } S = \frac{1}{2\eta} = \frac{1}{E_{LUMO} - E_{HOMO}} \quad (6)$$

As illustrated in table 4, the μ of the investigated chromophores increases in the following order: PTZ-4 (-4.47) < PTZ-3 (-4.35) < PTZ-2 (-4.31) (eV) < PTZ-1 (-4.30) (eV). The η indicates that the chromophores PTZ-1, PTZ-2, PTZ-3, and PTZ-4 have the lowest values, namely 0.81, 0.79, 0.66, and 0.83 (eV). Hence, they are soft molecules. Additionally, the χ values of the chromophores PTZ-1- PTZ-4 were determined to be 4.30, 4.31, 4.35, and 4.47 (eV). Finally, the S values for all examined chromophores increase in the following order: PTZ-4 (0.60) < PTZ-3 (0.75) < PTZ-2 (0.79) (eV) < PTZ-1 (0.81) (eV).

Table 4. The E_{HOMO}, E_{LUMO}, E_g, μ, η, S and χ.

Chromophore	E_{HOMO}(eV)	E_{LUMO}(eV)	Egap(eV)	μ	η	S	χ
PTZ-1	-5.177	-3.497	1.68	-4.30	0.81	0.61	4.30
PTZ-2	-5.104	-3.512	1.59	-4.31	0.79	0.63	4.31
PTZ-3	-5.101	-3.601	1.50	-4.35	0.75	0.66	4.35
PTZ-4	-5.082	-3.877	1.20	-4.47	0.60	0.83	4.47

3.6. NLO properties.

The usage of NLO compounds is prominent in signal processing, optical switches, communication technology, optical memory devices, etc. [4647]. The optical response is influenced by the entire molecule's electrical characteristics, which are also related to the nonlinear (β and γ) and linear responses (α, etc.). To illustrate the influence of various auxiliary acceptor Ai units over the NLO response properties of all chromophores studied, the α and β_{total} have been computed by the CAM-B3LYP functional with the 6-31G (d) basis set, and the acquired findings are detailed in Table 5. As seen in table 5, the average polarizability of the chromophores investigated (PTZ-1-PTZ-4) is 608.62, 879.10, 767.95, and 757.79 a.u, respectively. All studied chromophores exhibit notable transitions along the x-axis (αxx), and modifying the acceptor groups influences the polarization values. Indeed, the chromophore PTZ-4 has the lowest α, while the inclusion of the appropriate acceptor group, such as 2,3-dimethylthieno[3,4-b]pyrazine (PTZ-2), results in the highest average polarizability. The maximum value of α is indicated by the PTZ-2. Indeed, the values α for the investigated chromophores decrease in the following order: 879.10 > 767.95 > 757.79 > 608.62. In the case of first hyperpolarizability (βtot), Table 5 indicates that for all chromophores studied, hyperpolarizability values are 26029.23, 66723.38, 35960.23, and 13541.17 a.u for PTZ-1, PTZ-1, PTZ-1, and PTZ-1, respectively. Indeed, for all examined chromophores, the computed βtot decreases in the following order: PTZ-2 > PTZ-3> PTZ-1 > PTZ-4. The chromophore PTZ-4 (13541.17 (a.u)) has the lowest βtot value. On the other hand, it was discovered that the chromophores PTZ-2 with 2,3-dimethylthieno[3,4-b]pyrazine as acceptor unit has the highest βtot value of all molecules (66723.38 (a.u)). It can be observed that the NLO values of all molecules surpass those of urea, which is often used as a reference organic molecule (βtot value

of urea = 43 a.u) [48]. Generally, the data indicate that all compounds investigated possess polarizable properties.

Table 5. The average isotropic polarizability <α> and the first hyperpolarizability βtot of PTZ-1 - PTZ-4.

Parameters	PTZ-1	PTZ-2	PTZ-3	PTZ-4
αxx	1071.53	1605.65	1395.90	1397.96
αxy	-73.25	-175.16	147.711	-113.54
αyy	427.62	669.75	605.49	521.05
αxz	11.31	2.06	24.72	0.01
αyz	-13.64	8.51	-2.82	0.01
αzz	326.72	361.89	302.48	354.37
<α> (a.u)	608.62	879.10	767.95	757.79
βxxx	26571.50	-62213.90	-35116.60	-13345.00
βxxy	-2806.57	14664.80	-5219.07	-606.52
βxyy	-237.89	-3069.02	-646.70	-491.72
βyyy	408.82	309.36	26.434	-394.52
βxxz	610.76	-1021.56	-1075.07	-1.65
βxyz	-72.62	219.92	-289.22	0.43
βyyz	-22.82	158.21	176.44	0.06
βxzz	-410.74	314.19	187.34	314.79
βyzz	96.61	191.08	67.59	279.39
βzzz	-106.93	-180.72	-207.90	-0.17
β_{tot}(a.u)	26029.23	66723.38	35960.23	13541.17

3.7. Absorption properties.

3.7.1. Valuation of methodology.

The selection of the functional calculations is essential to precise the description of the vertical transition energy. Hence, the absorption wavelengths (λmax) of the reference chromophore (PTZ-1) in CH_3Cl solvent were tested by TD-DFT employing various hybrid density functionals PBEPBE [49], MPW97 [50], B3LYP [51], CAM-B3LYP [52] and WB97XD [53] with 6-31G (d,p) level [54] as indicated in table 6. The results indicate that the functional hybrid CAM-B3LYP with 6–31G (d,p) more closely matches the experimental value than the other functionals investigated (with a difference of approximately -45 nm). Based on the achieved findings, the CAM-B3LYP/ 6–31G (d,p) level has been chosen to compute the optical characteristics of the four proposed chromophores.

Table 6. Validation of the functional in the TD-DFT prediction of the λmax of the PTZ-1 in CH_3Cl solvent.

Theoretical methods	λmax (nm) / RE*
PBEPBE	1726.03/ 1194.03
B3PW91	767.31/ 235.31
mPW1PW91	674.72/ 142.72
B3LYP	767.31/ 235.31
CAM-B3LYP	486.94/ -45.06
WB97XD	478.33/ -54.67
Exp	532

Based on optimized ground-state geometries obtained by the B3LYP/6-31G (d,p) approach for all chromophores investigated, the optical characteristics such as the transition energy (Eex), the maximum absorption wavelength (λmax), the oscillator strength (*f*), major transitions (MO) and % contribution have been computed employing TD-DFT/CAM-B3LYP with 6–31G(d,p) basis set [5556] in various organic solvents. Table 7 contains the collected results, and Figure 6 shows the corresponding UV–visible spectrum. As shown in table 7 and fig. 6, theoretical data show that the absorption wavelength values of PTZ-1 range from 476.47 to 488.50 nm, while the absorption wavelength values of PTZ-2, PTZ-3, and PTZ-4 range from 519.19 to 605.86 nm in different organic solvents investigated. Furthermore, the S0 → S1

excitations of the molecules PTZ-1-PTZ-4 having the transition energy varies between 2.04 and 2.56 eV, and the oscillator strength between 2.12–2.36 is mainly contributed to HOMO → LUMO transitions (93%, 89%, 90%, and 81%, respectively). We observe that the TD-DFT data indicate that solvent polarity did not affect the absorption of the organic chromophores studied (PTZ-1-PTZ-4).

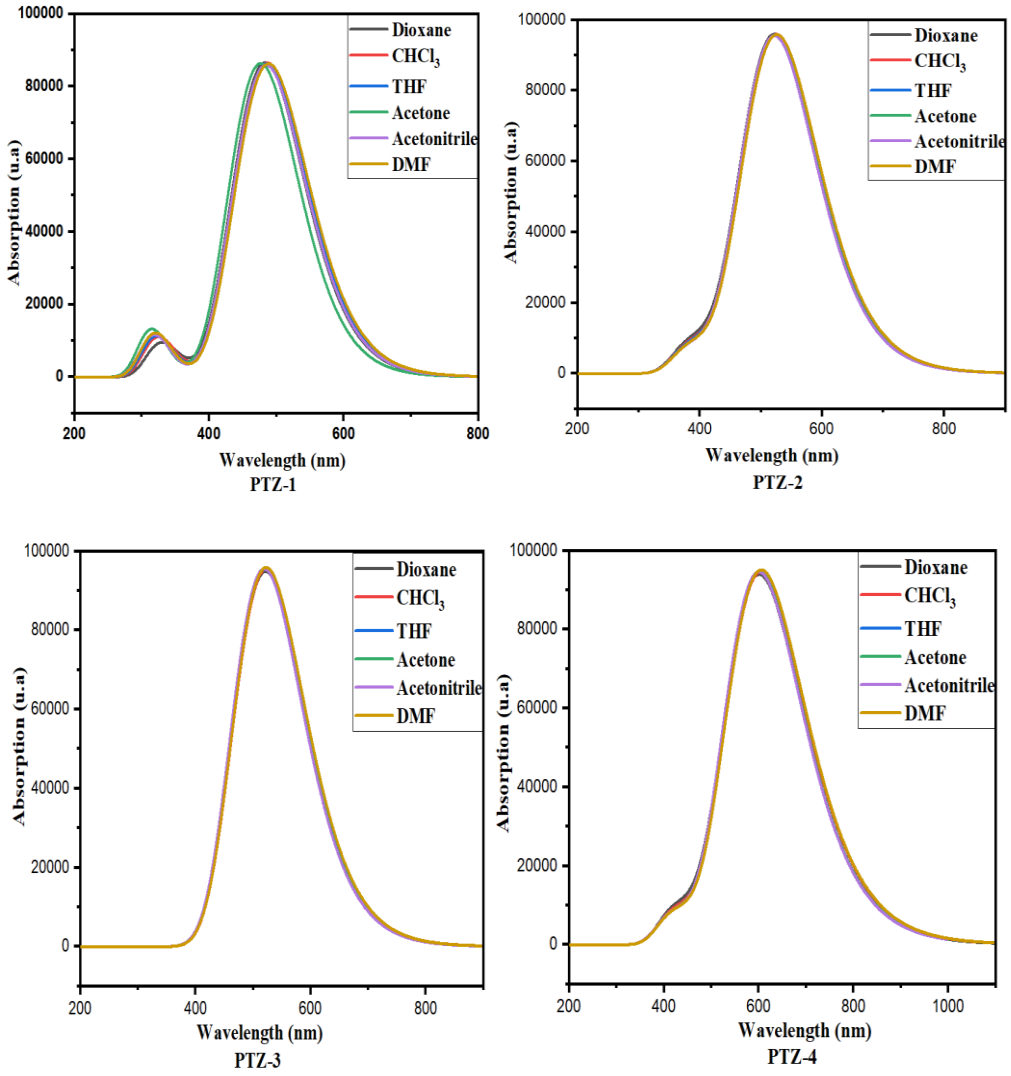

Figure 6. UV-vis spectrum of four chromophores PTZ-1- PTZ-4 in different solvents.

Table 7. Absorption spectra data calculated at TD-DFT/ CAM-B3LYP/6-31G (d,p) level.

Chromophore	Solvent	λ_{max} (nm)	Eex (eV)	*f*	MO/character	(%)
PTZ-1	Dioxane	483.403	2.56	2.13	HOMO -1->LUMO	(93%)
	Chloroform	486.93	2.54	2.23	HOMO -1->LUMO	(93%)
	THF	486.13	2.55	2.13	HOMO -1->LUMO	(93%)
	Acetone	476.47	2.60	2.13	HOMO -1->LUMO	(90%)
	Acetonitrile	484.59	2.55	2.12	HOMO -1->LUMO	(93%)
	DMF	488.50	2.53	2.13	HOMO -1->LUMO	(93%)
PTZ-2	Dioxane	568.93	2.37	2.36	HOMO -1->LUMO	(89%)
	Chloroform	525.15	2.36	2.36	HOMO -1->LUMO	(89%)
	THF	524.10	2.36	2.36	HOMO -1->LUMO	(89%)
	Acetone	522.73	2.37	2.35	HOMO -1->LUMO	(89%)
	Acetonitrile	522.21	2.37	2.35	HOMO -1->LUMO	(89%)
	DMF	526.04	2.36	2.36	HOMO -1->LUMO	(89%)
PTZ-3	Dioxane	521.83	2.37	2.34	HOMO -1->LUMO	(90%)
	Chloroform	522.84	2.36	2.35	HOMO -1->LUMO	(90%)
	THF	521.44	2.37	2.35	HOMO -1->LUMO	(90%)
	Acetone	519.75	2.37	2.35	HOMO -1->LUMO	(90%)

Chromophore	Solvent	λ_{max} (nm)	Eex (eV)	*f*	MO/character	(%)
	Acetonitrile	519.19	2.37	2.35	HOMO -1->LUMO	(90%)
	DMF	522.69	2.36	2.36	HOMO -1->LUMO	(90%)
PTZ-4	Dioxane	601.48	2.06	2.31	HOMO->LUMO	(81%)
	Chloroform	605.26	2.04	2.33	HOMO->LUMO	(81%)
	THF	603.64	2.05	2.33	HOMO->LUMO	(81%)
	Acetone	601.45	2.04	2.33	HOMO->LUMO	(81%)
	Acetonitrile	600.60	2.06	2.33	HOMO->LUMO	(81%)
	DMF	605.86	2.05	2.33	HOMO->LUMO	(81%)

4. Conclusions

This research designed phenothiazine-based organic chromophores having a D-Ai-π-A structure and investigated the potential effect of various auxiliary acceptors on their NLO characteristics. All studied chromophores showed maximum wavelengths λ_{max} in the visible region with small transition energy values. Our FMO analysis of PTZ-1, PTZ-2, PTZ-3, and PTZ-4 revealed that the chromophores' energy band gaps were reduced from 1.68 eV to 1.20 eV. Their NBO studies demonstrated that electrons could move successfully between D and A units. Due to the stronger auxiliary acceptors, the entitled chromophores (PTZ-2 and PTZ-3) demonstrated a more promising NLO response than the PTZ-1 reference chromophore. NLO responses leading to favorable < a> and βtot values with following order: PTZ-2 >PTZ-3 > PTZ-1 > PTZ-4. Generally, All chromophores with various auxiliary acceptors present a large NLO response ranging from 13541.17 to 66723.38 (a.u), PTZ-2 especially with auxiliary acceptor 2,3-dimethylthieno[3,4-b]pyrazine presents the highest <a> [(879.10 (a.u)) and βtot (66723.38 (a.u)] values. Eventually, it was concluded that entitled chromophores exhibited good NLO properties because their βtotal values were much greater than urea. The available data demonstrates that entitled compounds have fascinating NLO properties indicating that they are accomplished candidates for NLO material.

Funding

This research received no external funding.

Acknowledgments

This research has no acknowledgment.

Conflicts of Interest

The authors declare no conflict of interest.

References

1. Roucan, M.; Kielmann, M.; Connon, S.J.; Bernhard, S.S.R.; Senge, M.O. Conformational Control of Nonplanar Free Base Porphyrins: Towards Bifunctional Catalysts of Tunable Basicity. *Chem. Commun.* **2018**, *54*, 26–29, https://doi.org/10.1039/C7CC08099A.
2. Zhang, C.Z.; Lu, C.; Zhu, J.; Lu, G.Y.; Wang, X.; Shi, Z.W.; Liu, F.; Cui, Y. The Second-Order Nonlinear Optical Materials with Combined Nonconjugated D−π−A Units. *Chem. Mater.* **2006**, *18*, 6091–6093, https://doi.org/10.1021/cm0618042.
3. Khan, M.U.; Khalid, M.; Khera, R.A.; Akhtar, M.N.; Abbas, A.; Rehman, M.F.; Braga, A.A.C.; Alam, M.M.; Imran, M.; Wang, Y.; Lu, C. Influence of Acceptor Tethering on the Performance of Nonlinear Optical Properties for Pyrene-Based Materials with A-π-D-π-D Architecture. *Arabian Journal of Chemistry* **2022**, *15*, https://doi.org/10.1016/j.arabjc.2021.103673.
4. Shruthi, C.; Ravindrachary, V.; Guruswamy, B.; Prasad, D.J.; Goveas, J.; Kumara, K.; Lokanath, N.K. Molecular Structure, Hirshfeld Surface and Density Functional Theoretical Analysis of a NLO Active

Chalcone Derivative Single Crystal—A Quantum Chemical Approach. *Journal of Molecular Structure* **2021**, *1228*, https://doi.org/10.1016/j.molstruc.2020.129739.
5. Zhang, C.Z.; Lu, C.; Zhu, J.; Lu, G.Y.; Wang, X.; Shi, Z.W.; Liu, F.; Cui, Y. The Second-Order Nonlinear Optical Materials with Combined Nonconjugated D−π−A Units. *Chem. Mater.* **2006**, *18*, 6091–6093, https://doi.org/10.1021/cm0618042.
6. Hermet, P.; Fraysse, G.; Lignie, A.; Armand, P.; Papet, P. Density Functional Theory Predictions of the Nonlinear Optical Properties in α-Quartz-Type Germanium Dioxide. *J. Phys. Chem. C* **2012**, *116*, 8692–8698, https://doi.org/10.1021/jp300855q.
7. Abdel-Latif, S.A.; Moustafa, H. Synthesis, Spectroscopic Properties, Density Functional Theory Calculations and Nonlinear Optical Properties of Novel Complexes of 5-Hydroxy-4,7-Dimethyl-6-(Phenylazo)Coumarin with Mn(II), Co(II), Ni(II), Cu(II) and Zn(II) Metal Ions. *Appl Organometal Chem* **2018**, *32*, https://doi.org/10.1002/aoc.4269.
8. Sutradhar, T.; Misra, A. The Role of π-Linkers and Electron Acceptors in Tuning the Nonlinear Optical Properties of BODIPY-Based Zwitterionic Molecules. *RSC Adv.* **2020**, *10*, 40300–40309, https://doi.org/10.1039/D0RA02193H.
9. Arshad, M.N.; Khalid, M.; Ghulam shabbir; Asad, M.; Asiri, A.M.; Alotaibi, M.M.; Braga, A.A.C.; Khan, A. Donor Moieties with D–π–a Framing Modulated Electronic and Nonlinear Optical Properties for Non-Fullerene-Based Chromophores. *RSC Adv.* **2022**, *12*, 4209–4223, https://doi.org/10.1039/D1RA07183A.
10. Otero, R.; Vázquez de Parga, A.L.; Gallego, J.M. Electronic, Structural and Chemical Effects of Charge-Transfer at Organic/Inorganic Interfaces. *Surface Science Reports* **2017**, *72*, 105–145, https://doi.org/10.1016/j.surfrep.2017.03.001.
11. Wielopolski, M.; Kim, J.H.; Jung, Y.S.; Yu, Y.J.; Kay, K.Y.; Holcombe, T.W.; Zakeeruddin, S.M.; Grätzel, M.; Moser, J.-E. Position-Dependent Extension of π-Conjugation in D-π-A Dye Sensitizers and the Impact on the Charge-Transfer Properties. *J. Phys. Chem. C* **2013**, *117*, 13805–13815. https://doi.org/10.1021/jp402411h.
12. Zhang, Z.; Zhu, J.; Lv, Y.; Lan, A.; Lu, H.; Chen, F.; Huang, W. Explore Fused-Ring Core Incorporated A-π-D-π-A Type Acceptors and Their Application in Organic Solar Cells: Insight into Molecular Conformation, Optical and Electrochemical Properties, Film Morphology, and Energy Loss. *Dyes and Pigments* **2021**, *196*, https://doi.org/10.1016/j.dyepig.2021.109572.
13. Wu, Y.; Zhu, W.H.; Zakeeruddin, S.M.; Grätzel, M. Insight into D–A−π–A Structured Sensitizers: A Promising Route to Highly Efficient and Stable Dye-Sensitized Solar Cells. *ACS Appl. Mater. Interfaces* **2015**, *7*, 9307–9318, https://doi.org/10.1021/acsami.5b02475.
14. Wu, Y.; Zhu, W. Organic Sensitizers from D–π–A to D–A–π–A: Effect of the Internal Electron-Withdrawing Units on Molecular Absorption, Energy Levels and Photovoltaic Performances. *Chem. Soc. Rev.* **2013**, *42*, 2039–2058, https://doi.org/10.1039/C2CS35346F.
15. Li, W.; Wu, Y.; Zhang, Q.; Tian, H.; Zhu, W. D-A-π-A Featured Sensitizers Bearing Phthalimide and Benzotriazole as Auxiliary Acceptor: Effect on Absorption and Charge Recombination Dynamics in Dye-Sensitized Solar Cells. *ACS Appl. Mater. Interfaces* **2012**, *4*, 1822–1830, https://doi.org/10.1021/am3001049.
16. Yoosuf, M.; Pradhan, S.C.; Sruthi, M.M.; Soman, S.; Gopidas, K.R. Propellar Shaped Triple Bond Rigidified D-A-π-A Triphenylamine Dye as Back Electron Interceptor in Iodine and Cobalt Electrolyte DSSCs under Full Sun and Indoor Light. *Solar Energy* **2021**, *216*, 151–163, https://doi.org/10.1016/j.solener.2021.01.001.
17. Zhu, H.; Li, W.; Wu, Y.; Liu, B.; Zhu, S.; Li, X.; Ågren, H.; Zhu, W. Insight into Benzothiadiazole Acceptor in D–A−π–A Configuration on Photovoltaic Performances of Dye-Sensitized Solar Cells. *ACS Sustainable Chem. Eng.* **2014**, *2*, 1026–1034, https://doi.org/10.1021/sc500035j.
18. Hou, F.; Liu, X.; Hao, X.; Li, G.; Lu, F.; Deng, Q. New Benzotriazole-Based D–A–D Type Solvatochromic Dyes for Water Content Detection in Organic Solvents. *Dyes and Pigments* **2021**, *195*, https://doi.org/10.1016/j.dyepig.2021.109667.
19. Mao, J.; Guo, F.; Ying, W.; Wu, W.; Li, J.; Hua, J. Benzotriazole-Bridged Sensitizers Containing a Furan Moiety for Dye-Sensitized Solar Cells with High Open-Circuit Voltage Performance. *Chem. Asian J.* **2012**, *7*, 982–991. https://doi.org/10.1002/asia.201100967.
20. Kalinin, A.A.; Sharipova, S.M.; Levitskaya, A.I.; Dudkina, Y.B.; Burganov, T.I.; Fominykh, O.D.; Katsyuba, S.A.; Budnikova, Y.H.; Balakina, M. Yu. D-π-A'-π-A Chromophores with Quinoxaline Core in the π-Electron Bridge and Charged Heterocyclic Acceptor Moiety: Synthesis, DFT Calculations, Photophysical and Electro-Chemical Properties. *Journal of Photochemistry and Photobiology A: Chemistry* **2021**, *407*, https://doi.org/10.1016/j.jphotochem.2020.113042.
21. Yashwantrao, G.; Saha, S. Perspective on the Rational Design Strategies of Quinoxaline Derived Organic Sensitizers for Dye-Sensitized Solar Cells (DSSC). *Dyes and Pigments* **2022**, *199*, https://doi.org/10.1016/j.dyepig.2022.110093.
22. Zaier, R.; Ayachi, S. DFT Molecular Modeling Studies of D-π-A-π-D Type Cyclopentadithiophene-Diketopyrrolopyrrole Based Small Molecules Donor Materials for Organic Photovoltaic Cells. *Optik* **2021**, *239*, https://doi.org/10.1016/j.ijleo.2021.166787.
23. Raftani, M.; Abram, T.; Azaid, A.; Kacimi, R.; Bennani, M.N.; Bouachrine, M. Theoretical Design of New Organic Compounds Based on Diketopyrrolopyrrole and Phenyl for Organic Bulk Heterojunction Solar Cell

Applications: DFT and TD-DFT Study. *Materials Today: Proceedings* **2021**, *45*, 7334–7343, https://doi.org/10.1016/j.matpr.2020.12.1228.
24. Yang, Y.; Xu, W.; Zhao, J.; Liu, J. Using Phenothiazine as Electron Donor for New Second-Order Nonlinear Optical Chromophore. *Materials Letters* **2019**, *245*, 196–199, https://doi.org/10.1016/j.matlet.2019.02.096.
25. Khalid, M.; Ali, A.; Jawaria, R.; Asghar, M.A.; Asim, S.; Khan, M.U.; Hussain, R.; Fayyaz ur Rehman, M.; Ennis, C.J.; Akram, M.S. First Principles Study of Electronic and Nonlinear Optical Properties of A–D–π–A and D–A–D–π–A Configured Compounds Containing Novel Quinoline–Carbazole Derivatives. *RSC Adv.* **2020**, *10*, 22273–22283, https://doi.org/10.1039/D0RA02857F.
26. Frisch, M.; Trucks, G.W.; Schlegel, H.B.; Scuseria, G.E.; Robb, M.A.; Cheeseman, J.R.; Scalmani, G.; Barone, V.; Mennucci, B.; Petersson, G. Gaussian 09, Rev. A.02. **2009.**
27. R. Dennington, T. Keith, J. Millam, GaussView, version 5.0 (Semichem Inc., Shawnee, **2005**).
28. Lee, C.; Yang, W.; Parr, R.G. Development of the Colle-Salvetti Correlation-Energy Formula into a Functional of the Electron Density. *Phys. Rev. B* **1988**, *37*, 785–789, https://doi.org/10.1103/PhysRevB.37.785.
29. Govindharajan, G.; Jeyaseelan, S.; Pari, S.; Febena, A.S. Structural, Optical, FT-IR and SHG Studies of L-Isoleucine D-Valine: A Spectroscopic and DFT Approach. *Materials Today: Proceedings* **2022**, *50*, 2627–2631, https://doi.org/10.1016/j.matpr.2020.07.477.
30. Tasgin, D.I.; Sirin, P.S. A Theoretical Investigation: Effect of Structural Modifications on Molecular, Electronic, and Optical Properties of Phosphonate Substituted BODIPY Dyes. *ChemistrySelect* **2021**, 6, 4677–4683, https://doi.org/10.1002/slct.202100821.
31. Łapczuk-Krygier, A.; Kącka-Zych, A.; Kula, K. Recent Progress in the Field of Cycloaddition Reactions Involving Conjugated Nitroalkenes. *Current Chemistry Letters* **2019**, *8*, 13–38, https://doi.org/10.5267/j.ccl.2018.12.002.
32. Foster, J.P.; Weinhold, F. Natural Hybrid Orbitals. *J. Am. Chem. Soc.* **1980**, *102*, 7211–7218, https://doi.org/10.1021/ja00544a007.
33. Guillaumont, D.; Nakamura, S. Calculation of the Absorption Wavelength of Dyes Using Time-Dependent Density-Functional Theory (TD-DFT). *Dyes and Pigments* **2000**, *46*, 85–92, https://doi.org/10.1016/S0143-7208(00)00030-9.
34. Yanai, T.; Tew, D.P.; Handy, N.C. A New Hybrid Exchange–Correlation Functional Using the Coulomb-Attenuating Method (CAM-B3LYP). *Chemical Physics Letters* **2004**, *393*, 51–57, https://doi.org/10.1016/j.cplett.2004.06.011.
35. Lin, C.; Wu, K. Theoretical Studies on the Nonlinear Optical Susceptibilities of 3-Methoxy-4-Hydroxy-Benzaldehyde Crystal. *Chemical Physics Letters* **2000**, *321*, 83–88, https://doi.org/10.1016/S0009-2614(00)00323-7.
36. Ghanavatkar, C.W.; Mishra, V.R.; Sekar, N. Review of NLOphoric Azo Dyes – Developments in Hyperpolarizabilities in Last Two Decades. *Dyes and Pigments* **2021**, *191*, https://doi.org/10.1016/j.dyepig.2021.109367.
37. Kacimi, R.; Bourass, M.; Toupance, T.; Wazzan, N.; Chemek, M.; El Alamy, A.; Bejjit, L.; Alimi, K.; Bouachrine, M. Computational Design of New Organic (D–π–A) Dyes Based on Benzothiadiazole for Photovoltaic Applications, Especially Dye-Sensitized Solar Cells. *Res Chem Intermed* **2020**, *46*, 3247–3262, https://doi.org/10.1007/s11164-020-04150-7.
38. Mao, J.; Guo, F.; Ying, W.; Wu, W.; Li, J.; Hua, J. Benzotriazole-Bridged Sensitizers Containing a Furan Moiety for Dye-Sensitized Solar Cells with High Open-Circuit Voltage Performance. *Chem. Asian J.* **2012**, *7*, 982–991, https://doi.org/10.1002/asia.201100967.
39. Bourass, M.; Touimi Benjelloun, A.; Benzakour, M.; Mcharfi, M.; Jhilal, F.; Serein-Spirau, F.; Marc Sotiropoulos, J.; Bouachrine, M. DFT/TD-DFT Characterization of Conjugational Electronic Structures and Spectral Properties of Materials Based on Thieno[3,2-b][1]Benzothiophene for Organic Photovoltaic and Solar Cell Applications. *Journal of Saudi Chemical Society* **2017**, *21*, 563–574, https://doi.org/10.1016/j.jscs.2017.01.001.
40. Luque, F.J.; López, J. M.; Orozco, M. Perspective on "Electrostatic Interactions of a Solute with a Continuum. A Direct Utilization of Ab Initio Molecular Potentials for the Prevision of Solvent Effects." *Theoretical Chemistry Accounts: Theory, Computation, and Modeling (Theoretica Chimica Acta)* **2000**, *103*, 343–345, https://doi.org/10.1007/s002149900013.
41. Raftani, M.; Abram, T.; Loued, W.; Kacimi, R.; Azaid, A.; Alimi, K.; Bennani, M.N.; Bouachrine, M. The Optoelectronic Properties of π-Conjugated Organic Molecules Based on Terphenyl and Pyrrole for BHJ Solar Cells: DFT/TD-DFT Theoretical Study. *Current Chemistry Letters* **2021**, *10*, 489–502, https://doi.org/10.5267/j.ccl.2021.4.002.
42. Mulliken, R.S. Electronic Structures of Molecules XI. Electroaffinity, Molecular Orbitals and Dipole Moments. *The Journal of Chemical Physics* **1935**, *3*, 573–585, https://doi.org/10.1063/1.1749731.
43. Islam, N.; Ghosh, D.C. On the Electrophilic Character of Molecules Through Its Relation with Electronegativity and Chemical Hardness. *nt. J. Mol. Sci.* **2012**, *13*, 2160–2175, https://doi.org/10.3390/ijms13022160.

44. Parr, R.G.; Pearson, R.G. Absolute Hardness: Companion Parameter to Absolute Electronegativity. *J. Am. Chem. Soc.* **1983**, *105*, 7512–7516, https://doi.org/10.1021/ja00364a005.
45. Parr, R.G.; Donnelly, R.A.; Levy, M.; Palke, W.E. Electronegativity: The Density Functional Viewpoint. *The Journal of Chemical Physics* **1978**, *68*, 3801–3807, https://doi.org/10.1063/1.436185.
46. Khan, M.U.; Khalid, M.; Ibrahim, M.; Braga, A.A.C.; Safdar, M.; Al-Saadi, A.A.; Janjua, M.R.S.A. First Theoretical Framework of Triphenylamine–Dicyanovinylene-Based Nonlinear Optical Dyes: Structural Modification of π-Linkers. *J. Phys. Chem. C* **2018**, *122*, 4009–4018, https://doi.org/10.1021/acs.jpcc.7b12293.
47. Arivuoli, D. Fundamentals of Nonlinear Optical Materials. *Pramana - J Phys* **2001**, *57*, 871–883, https://doi.org/10.1007/s12043-001-0004-1.
48. Mehmood, H.; Khalid, M.; Haroon, M.; Akhtar, T.; Ashfaq, M.; Tahir, M.N.; Khan, M.U.; Imran, M.; Braga, A.A.C.; Woodward, S. Synthesis, Characterization and DFT Calculated Properties of Electron-Rich Hydrazinylthiazoles: Experimental and Computational Synergy. *Journal of Molecular Structure* **2021**, *1245*, https://doi.org/10.1016/j.molstruc.2021.131043.
49. Perdew, J.P.; Burke, K.; Ernzerhof, M. Generalized Gradient Approximation Made Simple. *Phys. Rev. Lett.* **1996**, *77*, 3865–3868, https://doi.org/10.1103/PhysRevLett.77.3865.
50. Govindarajan, M.; Ganasan, K.; Periandy, S.; Mohan, S. DFT (LSDA, B3LYP and B3PW91) Comparative Vibrational Spectroscopic Analysis of α-Acetonaphthone. *Spectrochimica Acta Part A: Molecular and Biomolecular Spectroscopy* **2010**, *76*, 12–21, https://doi.org/10.1016/j.saa.2010.02.029.
51. Lee, C.; Yang, W.; Parr, R.G. Development of the Colle-Salvetti Correlation-Energy Formula into a Functional of the Electron Density. *Phys. Rev. B* **1988**, *37*, 785–789, https://doi.org/10.1103/PhysRevB.37.785.
52. Yanai, T.; Tew, D.P.; Handy, N.C. A New Hybrid Exchange–Correlation Functional Using the Coulomb-Attenuating Method (CAM-B3LYP). *Chemical Physics Letters* **2004**, *393*, 51–57, https://doi.org/10.1016/j.cplett.2004.06.011.
53. Chai, J.-D.; Head-Gordon, M. Long-Range Corrected Hybrid Density Functionals with Damped Atom–Atom Dispersion Corrections. *Phys. Chem. Chem. Phys.* **2008**, *10*, https://doi.org/10.1039/b810189b.
54. Becke, A.D. A New Mixing of Hartree–Fock and Local Density-functional Theories. *The Journal of Chemical Physics* **1993**, *98*, 1372–1377, https://doi.org/10.1063/1.464304.
55. Zaitri, L.K.; Mekelleche, S.M. DFT and TD-DFT Study on Quadratic NLO Response and Optoelectronic Activity in Novel Y-Shaped Imidazole-Based Push-Pull Chromophores. *Journal of Molecular Modeling* **2021**, https://doi.org/10.21203/rs.3.rs-197164/v1.
56. Khalid, M.; Khan, M.U.; Shafiq, I.; Hussain, R.; Mahmood, K.; Hussain, A.; Jawaria, R.; Hussain, A.; Imran, M.; Assiri, M.A.; Ali, A.; ur Rehman, M.F.; Sun, K.; Li, Y. NLO Potential Exploration for D–π–A Heterocyclic Organic Compounds by Incorporation of Various π-Linkers and Acceptor Units. *Arabian Journal of Chemistry* **2021**, *14*, https://doi.org/10.1016/j.arabjc.2021.103295.